

This article was downloaded by: [Pontificia Universidad Javeria]

On: 24 August 2011, At: 13:24

Publisher: Taylor & Francis

Informa Ltd Registered in England and Wales Registered Number: 1072954 Registered office: Mortimer House, 37-41 Mortimer Street, London W1T 3JH, UK



Supramolecular Chemistry

Publication details, including instructions for authors and subscription information:

<http://www.tandfonline.com/loi/gsch20>

Remote chiral transfer into [2+2] and [2+4] cycloadditions within self-assembled molecular flasks

Takashi Murase^a, Stéphane Peschard^a, Shinnosuke Horiuchi^a, Yuki Nishioka^a & Makoto Fujita^{a,b}

^a Department of Applied Chemistry, School of Engineering, The University of Tokyo, Hongo, Bunkyo-ku, Tokyo, 113-8656, Japan

^b Core Research for Evolutional Science and Technology (CREST), Japan Science and Technology Agency (JST), Hongo, Bunkyo-ku, Tokyo, 113-8656, Japan

Available online: 13 Apr 2011

To cite this article: Takashi Murase, Stéphane Peschard, Shinnosuke Horiuchi, Yuki Nishioka & Makoto Fujita (2011): Remote chiral transfer into [2+2] and [2+4] cycloadditions within self-assembled molecular flasks, *Supramolecular Chemistry*, 23:03-04, 199-208

To link to this article: <http://dx.doi.org/10.1080/10610278.2010.521833>

PLEASE SCROLL DOWN FOR ARTICLE

Full terms and conditions of use: <http://www.tandfonline.com/page/terms-and-conditions>

This article may be used for research, teaching and private study purposes. Any substantial or systematic reproduction, re-distribution, re-selling, loan, sub-licensing, systematic supply or distribution in any form to anyone is expressly forbidden.

The publisher does not give any warranty express or implied or make any representation that the contents will be complete or accurate or up to date. The accuracy of any instructions, formulae and drug doses should be independently verified with primary sources. The publisher shall not be liable for any loss, actions, claims, proceedings, demand or costs or damages whatsoever or howsoever caused arising directly or indirectly in connection with or arising out of the use of this material.

Remote chiral transfer into [2 + 2] and [2 + 4] cycloadditions within self-assembled molecular flasks

Takashi Murase^a, Stéphane Peschard^a, Shinnosuke Horiuchi^a, Yuki Nishioka^a and Makoto Fujita^{ab*}

^aDepartment of Applied Chemistry, School of Engineering, The University of Tokyo, Hongo, Bunkyo-ku, Tokyo 113-8656, Japan;

^bCore Research for Evolutional Science and Technology (CREST), Japan Science and Technology Agency (JST),
Hongo, Bunkyo-ku, Tokyo 113-8656, Japan

(Received 5 July 2010; final version received 15 August 2010)

A self-assembled chiral coordination cage was prepared from triangular triazine-panel ligands and Pd(II) complexes with chiral diamine auxiliaries. The chiral environment of the cage is induced by the structural deformation of the triazine panels ascribed to the steric bulk of the substituents on the chiral auxiliaries. The chiral cage can accommodate a pair of two hydrophobic molecules to form a specific diastereomeric ternary complex. We succeeded in conducting unusual [2 + 2] and [2 + 4] asymmetric cycloadditions from the identical ternary complex including a maleimide derivative and aromatic compounds with 6–50% enantiomeric excess (ee). It is remarkable that the remote chirality on the auxiliaries is efficiently transmitted to the chiral orientation of achiral ligands, which define a chiral cavity, to induce up to 50% ee. The present strategy is widely applicable to cavity-directed asymmetric reactions and maintaining inherent properties of the cage.

Keywords: self-assembly; host–guest systems; pericyclic reaction; enantioselectivity; chiral transfer

Introduction

Asymmetric synthesis within chiral molecular flasks is one of the most interesting challenges in organic synthesis because such reactions mimic highly efficient and selective chemical transformations in the chiral cavities of enzymes (1–3). As an enzyme model, cyclodextrins offer chiral hydrophobic cavities derived from their inherent chirality of D-glucopyranoside units and mediate a variety of asymmetric reactions within the cavities (4–15). The host cavities transfer the chiral information through space to the accommodated prochiral substrates to direct the reactions in an enantioselective manner. This strategy is distinguished from chiral auxiliary strategy in which the chiral information is transferred through bonds to the connected, adjacent reaction sites (16–21). However, asymmetric synthesis within artificial chiral cavities remained relatively unexplored because of the difficulties in preparing and isolating optically pure forms of molecular flasks. Raymond et al. (22) have succeeded in resolving two enantiomeric forms of a tetrahedral coordination cage by encapsulating a chiral guest molecule. They employed the tetrahedral chiral cavity, to demonstrate that the catalytic 3-aza-Cope rearrangements of allyl enammonium cations are promoted highly enantioselectively within the cavity (23–25). Upon encapsulating the substrates, the cage asymmetrically induces the substrate

preorganisation to reduce the entropic cost of the rearrangement.

Chiral environment can also be created by attaching chiral auxiliaries to achiral cage frameworks or encapsulating a (small) chiral guest to render the remaining cavities chiral. Rebek et al. (26–30) proved that the remote stereocentres on chiral auxiliaries affect the behaviours of achiral guest molecules in the cavity of a hydrogen-bonded cylindrical capsule. The guests can feel the surrounding asymmetric environment beyond the cage framework. This phenomenon verifies that outer remote chiral information is transmitted through space to guests and that asymmetric reactions can be induced within the cavity.

We have used the chiral cavity of self-assembled M₆L₄ coordination cage **1** and have succeeded in promoting asymmetric [2 + 2] cross-photoadditions of fluoranthene (**2a**) with *N*-cyclohexylmaleimide (**3**) (Figure 1) (31). The chiral environment arises from the stereogenic centres of the chiral *trans*-diamine auxiliaries which are far from the central cavity. We presume that this chirality is once transferred to the chirality on the amino nitrogen atoms coordinating to Pd(II) centres and subsequently transferred into the chiral orientation of the achiral ligands. The remote chiral auxiliaries induce only a minor chiral deformation of the *T*-symmetric cavity surrounded by triazine panels. Nevertheless, such a slight chiral deformation is sufficient to

*Corresponding author. Email: mfujita@appchem.t.u-tokyo.ac.jp

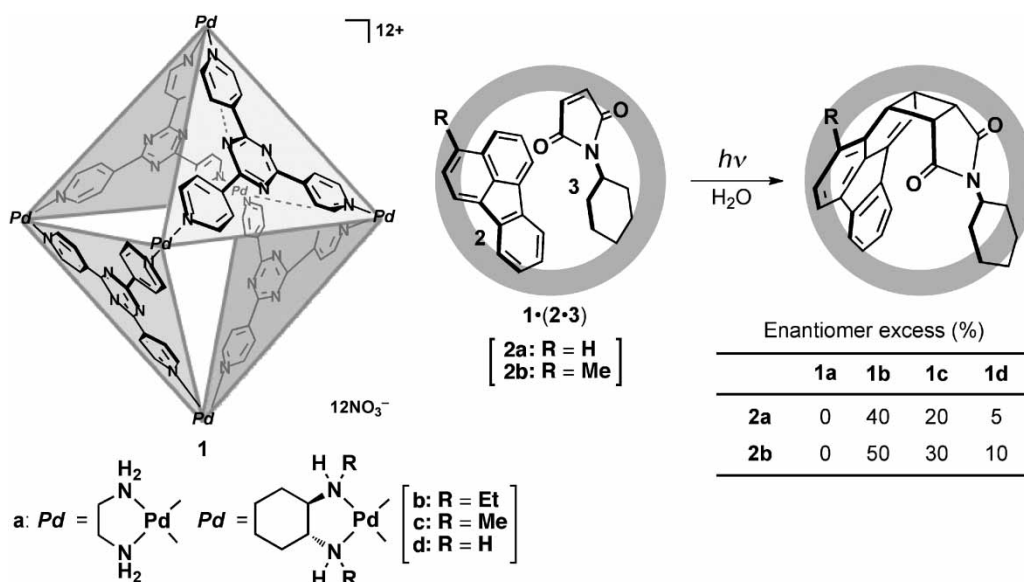


Figure 1. [2 + 2] asymmetric cross-photoadditions of fluoranthenes **2** with maleimide **3** within cage **1**.

induce moderate to high enantiomeric excess (ee) during chemical transformations in the cavity: up to 50% ee was achieved in the [2 + 2] photoaddition of maleimide **3** with 3-methyl fluoranthene (**2b**) (*31*). This chiral transfer strategy should be applicable to a variety of cavity-directed asymmetric reactions. In this study, we show asymmetric induction of both [2 + 2] photoadditions and [2 + 4] Diels–Alder reactions of inert aromatic compounds, aceanthrylene (**4**) and 1*H*-cyclopenta[*l*]phenanthrene (**5**), via identical host–guest complexes, using the chiral cavity of cage **1** (Figure 2) (*32*). All the above reactions proceed in regio-, stereo- and enantioselective manners.

Results and discussion

Substituent effects of chiral auxiliaries on cage **1**

Before performing cavity-directed asymmetric reactions, we clarified the substituent effects of chiral *trans*-cyclohexanediamine auxiliaries on cage **1** and investigated the deformation of the triazine panel, which is represented by the tilt angle α of the pyridine rings on the triazine panel (Figure 3(a)). Molecular mechanics calculation of cage **1** predicted that the tilt angle of the pyridine rings increased with increasing steric bulk, R [H (5°) < Me (13°) < Et (17°) < *i*-Pr (30°)]. In fact, the intensity of CD spectra of chiral cages increased in the

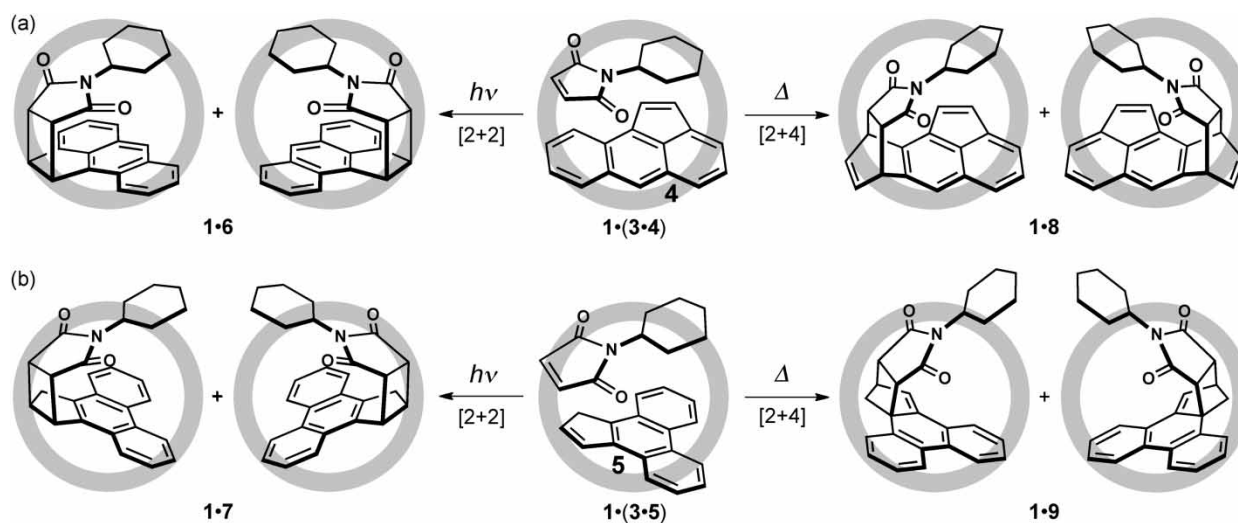


Figure 2. [2 + 2] and [2 + 4] cycloadditions of maleimide **3** with (a) aceanthrylene (**4**) and (b) 1*H*-cyclopenta[*l*]phenanthrene (**5**). Enantiomers of cycloadducts **6–9** are shown for each reaction.

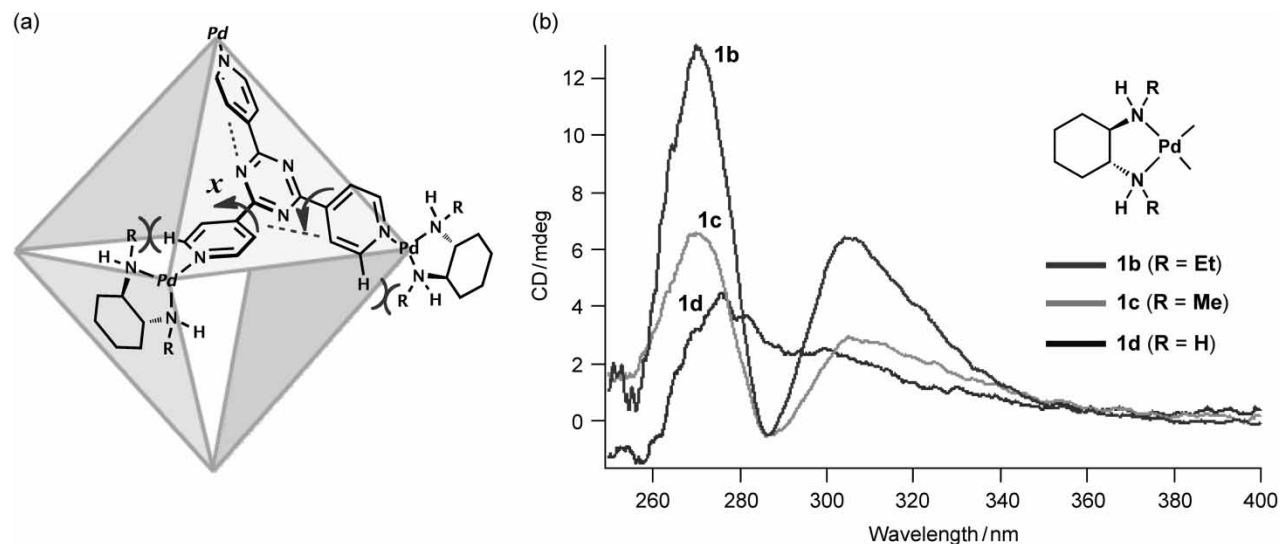


Figure 3. (a) The deformation of the triazine panels in cage **1** and the tilt angle, x , of the pyridine rings, and (b) CD spectra of cages **1b–d** (0.05 mM) in H₂O at room temperature (1 mm cell).

order of $H < Me < Et$ for the R group on the chiral auxiliaries, suggesting the chirality transmission from the auxiliaries to the cavity via Pd(II)-coordinated amino group having the R group (Figure 3(b)). Unfortunately, the cage with isopropyl chiral auxiliaries ($R = i\text{-Pr}$) failed to self-assemble because of too large steric hindrance of the substituents, though more efficient chiral induction was expected from the predicted tilt angle (30°). It is found that *trans*- N,N' -diethylcyclohexanediamine is the best chiral-inducing ligand for asymmetric deformation of M_6L_4 cages. Actually, chiral cage **1b** ($R = Et$) gave the highest ee value for the asymmetric [2 + 2] photoadditions of fluoranthenes **2** with **3**, as already demonstrated previously (31). Therefore, we used chiral cage **1b** for the following asymmetric reactions.

Pairwise encapsulation of guest molecules within cage 1

As aromatic guest molecules, we chose **4** and **5** for the following two reasons: (i) they give enantiomeric products on the cycloadditions with maleimide **3** and (ii) they are the same four-ring aromatic compounds as **2**, which allows us to roughly compare their asymmetric reactions within cage **1**, not considering their molecular sizes. Large planar aromatics and round-shaped molecules tend to be pair-wisely encapsulated within cage **1** to form ternary complexes (33). For example, when **3** and **4** were suspended in an aqueous solution of cage **1** at room temperature for 1 h, ternary complex **1**·(**3**·**4**) was obtained in 50% yield, as monitored by ¹H NMR (Figure 4(a))¹. The proton signals of both guests **3** and **4** were highly upfield shifted due to the encapsulation within cage **1**. Since the chiral centre of the auxiliary is located outside cage **1**, there were no significant differences in the guest-encapsulation properties between

chiral and achiral cages. In the same manner, ternary complex **1**·(**3**·**5**) was formed in 30% yields.

[2 + 2] cycloadditions (cross-photoadditions)

First, we carried out [2 + 2] photo-cycloadditions of aromatic compounds in the cavity of achiral cage **1a** to ensure their reactivity and obtain the racemic products as references. Some aromatic compounds which otherwise show no photo-reactivity can participate in [2 + 2] photoadditions when they are co-encapsulated with maleimide **3** in the cage. When ternary complex **1a**·(**3**·**4**) was irradiated with a high-pressure mercury lamp (400 W) at room temperature for 1 h, a single product **6** was obtained in 60% yield, as determined by the ¹H NMR spectrum (Figure 4(b)).² Because of the tight packing of the adduct in the host cage, the decomposition of the cage by hydrochloric acid was necessary to extract product **6** with chloroform. The reaction was very clean and no by-products were detected after the extraction (Figure 4(c)). The product analysis by NMR showed the exclusive formation of **6** with the *syn* stereochemistry.

The geometry of adduct **6** in the cage was clearly revealed by X-ray crystallographic analysis (Figure 5). A single crystal suitable for X-ray analysis was obtained by slow evaporation of water from an aqueous solution of the inclusion complex of adduct **6** over 1 week. As expected, the crystal structure showed the adduct with *syn* conformation, emphasising the snug fitting of **6** within the cage.

After establishing that cage **1** promotes the specific photoaddition of **4**, then asymmetric induction within a chiral cavity was examined. A similar ternary complex **1b**·(**3**·**4**) was obtained by mixing chiral cage **1b** with **3** and **4** in water. Upon photo-irradiation, photoadduct **6** was

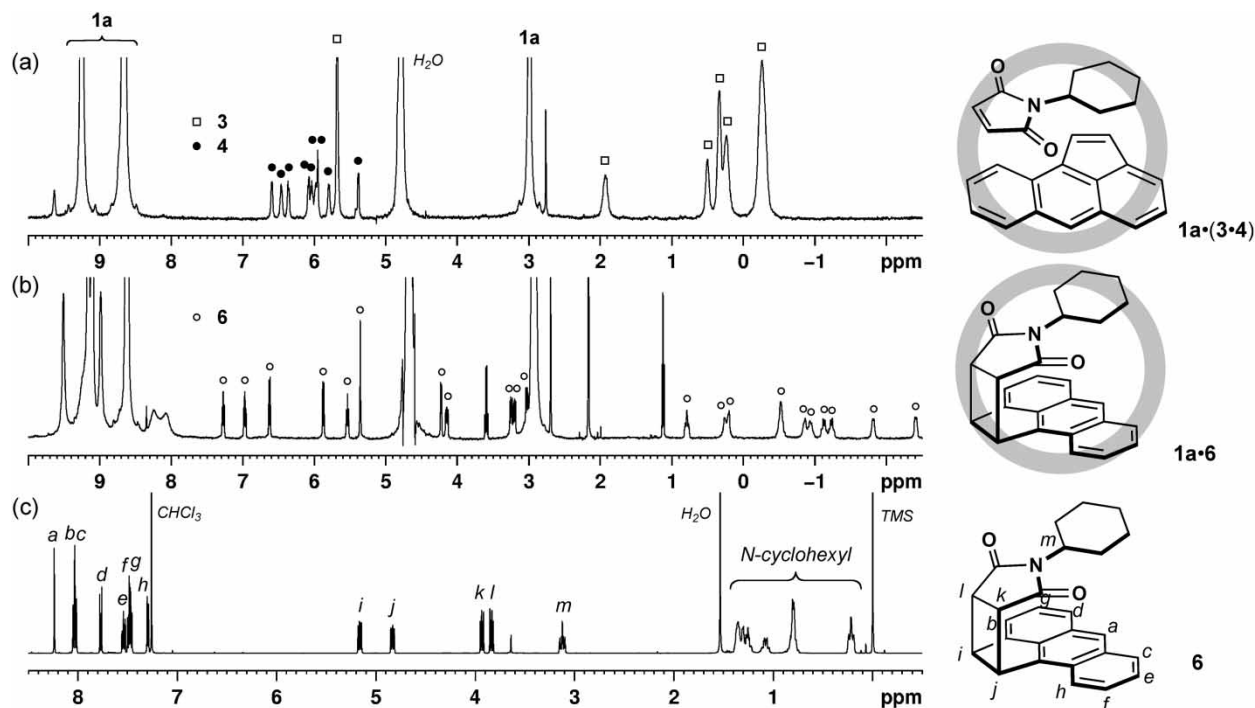


Figure 4. ^1H NMR spectra (500 MHz, 300 K) of (a) ternary complex **1a**·(**3**·**4**) (in D_2O), (b) product **1a**·**6** (in D_2O) and (c) photoadduct **6** (in CDCl_3).

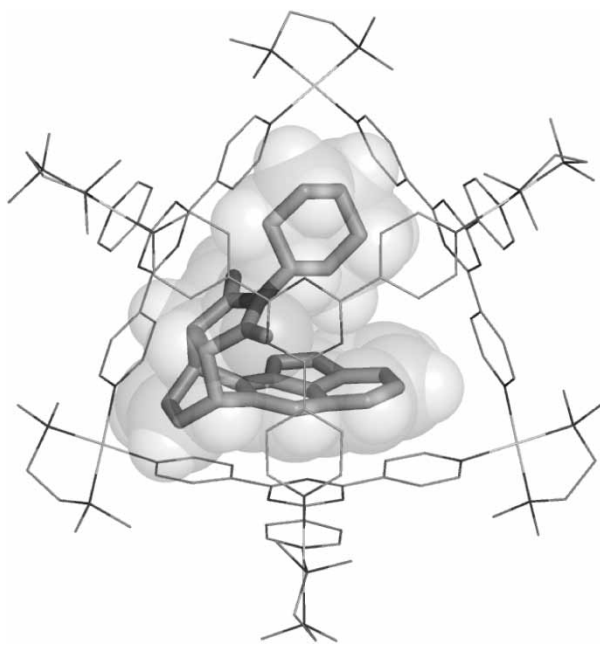


Figure 5. Crystal structure of the inclusion complex of adduct **6**. To obtain a good crystal, $(\text{tmeda})\text{Pd}(\text{NO}_3)_2$ was employed instead of $(\text{en})\text{Pd}(\text{NO}_3)_2$ in the formation of the cage. For clarity, H atom, anions and solvent molecules have been omitted. One of the two enantiomers is shown here. Four molecules of product **6** were equally disordered above each triazine panel ligand after symmetry operation (CCDC 777611).

formed again. Chiral HPLC analyses were conducted for the enantiomers obtained in achiral cage **1a** and chiral cage **1b** (Figure 6). Although there was of course no enantioselectivity in the case of achiral cage **1a**, the contrast of the peak area for enantiomers proved that the reaction proceeded with 44% ee within chiral cage **1b**.

We have not yet determined the absolute configuration of each enantiomer but confirmed that the ratio of the enantiomers was inverted when using chiral cage **1b'** with the opposite chiral auxiliary to cage **1b'** (Figure 6(c)). The enantiomers of **6** derive from the position of the projecting terminal benzene ring in the resulting anthracene moiety after the photoaddition. Thus, the deformation of the triazine panel in the cage causes the preferential recognition of either diastereomeric orientation of the substrate pair **3** and **4** within the cage. Although the rapid interconversion between two orientations is unable to distinguish the diastereomeric pair on the NMR timescale, it is no doubt that the position of the terminal benzene ring of **4** plays a significant role in the asymmetric reaction within chiral cage **1b**.

Similarly, a single regio- and stereo-isomer was obtained in the [2 + 2] photoaddition between **3** and **5**. When ternary complex **1a**·(**3**·**5**) was irradiated (400 W) at room temperature for 15 min, a single photoadduct **7** was obtained in 50% yield. Eight protons of the resulting phenanthrene core and four protons of the cyclobutane skeleton were observed in the ^1H NMR spectrum, which signifies the

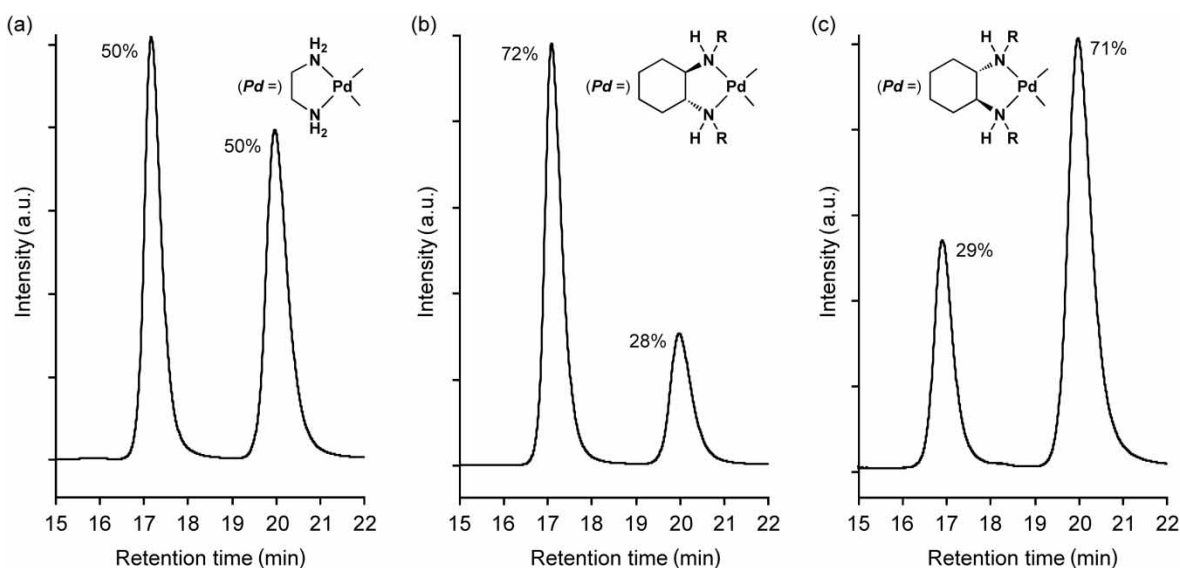


Figure 6. The HPLC analyses of photoadduct **6** formed inside (a) achiral cage **1a**, (b) chiral cage **1b** and (c) chiral cage **1b'** (with opposite chiral auxiliary to cage **1b**). The ratios of peak areas are shown for each chromatogram.

asymmetric structure of **7**. In the chiral cavity of cage **1b**, the photoreaction furnished the [2 + 2] adduct **7** with 33% ee.

[2 + 4] cycloadditions (Diels–Alder reactions)

Next, we focused on [2 + 4] cycloadditions (Diels–Alder reactions) of aromatic compounds. In the hydrophobic

cavity of the cage, aromatic compounds **4** and **5** showed not only photo-reactivity but also Diels–Alder reactivity via identical ternary complexes. When ternary complex **1a**·(**3**·**4**) was heated at 100°C for 1 h, the signals derived from guests **3** and **4** completely disappeared, and a set of new signals appeared in the ¹H NMR spectrum (Figure 7(b)). The signal integration indicated that 90% of

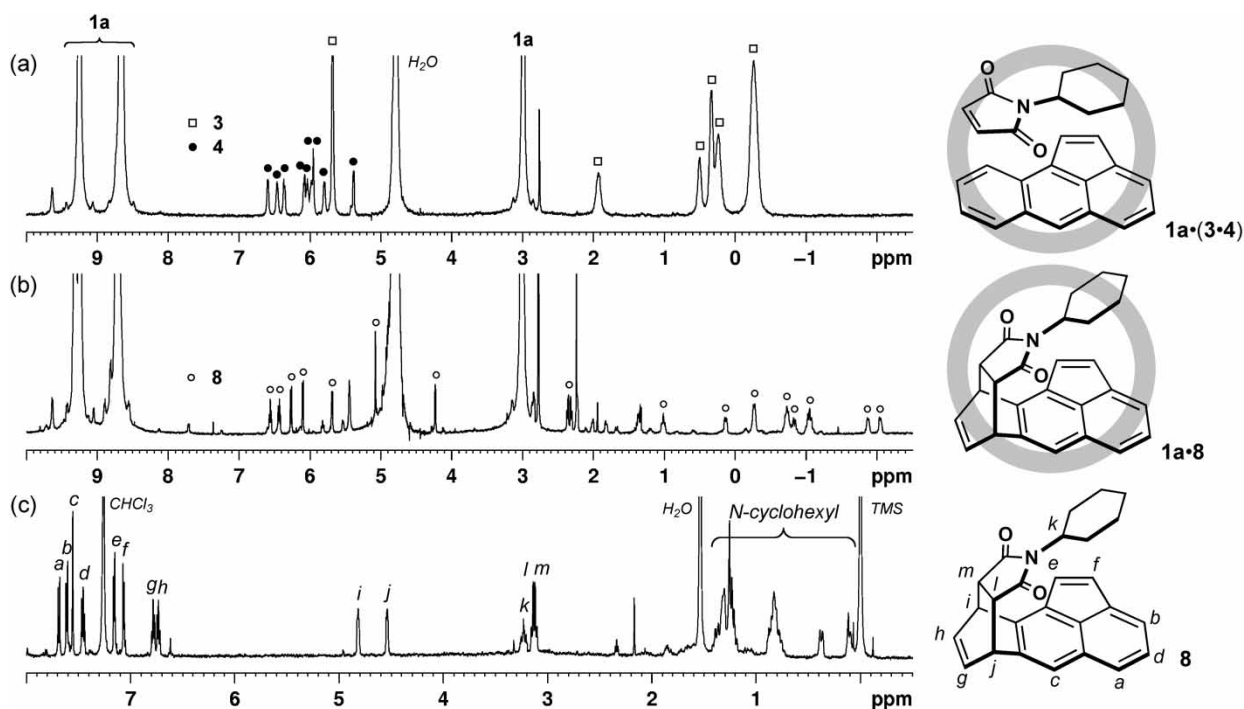


Figure 7. ¹H NMR spectra (500 MHz, 300 K) of (a) ternary complex **1a**·(**3**·**4**) (in D₂O), (b) product **1a**·**8** (in D₂O) and (c) Diels–Alder adduct **8** (in CDCl₃).

encapsulated **4** was converted to Diels–Alder adduct **8**. The adduct was extracted with chloroform after the decomplexation of the cage by hydrochloric acid and analysed by NMR spectroscopy and mass spectrometry (Figure 7(c)). The reaction was regio-selective at the protruding terminal benzene ring of **4**, in an *exo*-selective fashion. The *syn* stereochemistry was revealed by the shielding of *N*-cyclohexyl protons due to the neighbouring acenaphthylene core.

The structure of **8** was ultimately confirmed by X-ray crystallographic analysis (Figure 8). Because of the steric demand of the *N*-cyclohexyl group, dienophile **3** is allowed only to access the terminal benzene ring of **4**, and the compact *syn*-isomer is just fitted in the cavity of the cage. Thus, both regio- and stereo-selectivities were perfectly controlled in the reaction of an otherwise unreactive substrate.

When chiral cage **1b** was employed for the above Diels–Alder reaction, 6% ee of **8** was achieved. The 6% ee value is remarkable considering that the reaction was carried out at 100°C and that the chiral auxiliary is located on the peripheral positions of the cage. Because the chirality of the cavity arises from the deformation of the triazine panel caused by the steric hindrance of the substituents on the

remote chiral auxiliary, such a deformation could be usually relieved by the free rotation of the pyridine rings at 100°C. This result proves that the chiral information of the auxiliary ligand is remotely transferred to the cavity of the cage through bonds even at high temperature.

Although compound **5** has been attracted as a ligand in the preparation of a series of metallocenes with phenanthrene frameworks (34, 35), the Diels–Alder reaction of **5** is very sluggish even at 130°C for 3 days (36). However, in the cavity of cage **1**, the Diels–Alder reaction is efficiently promoted, as a consequence of high effective concentration and substrate preorganisation within the cage. When ternary complex **1a**·(**3**·**5**) was heated at 100°C for 1 h, the Diels–Alder adduct **9** was formed in 95% yield with 100% *syn* stereoselectivity. The same reaction proceeded in the chiral cavity of cage **1b**, and to our surprise, the ee value was found to be 26% by chiral HPLC analysis. Compared to adduct **8**, the configuration difference between both enantiomers is large in adduct **9**, which is supposed to be much affected by the chiral cavity of the cage and leads to the better ee value.

Comparison of [2 + 2] and [2 + 4] cycloadditions within chiral cage **1b**

Enantioselectivity of [2 + 2] and [2 + 4] cycloadditions of aromatics with maleimide **3** within chiral cage **1b** is summarised in Table 1. In general, enantioselectivity of [2 + 2] photoadditions was higher than that of [2 + 4] thermal-additions, but the difference of the ee values

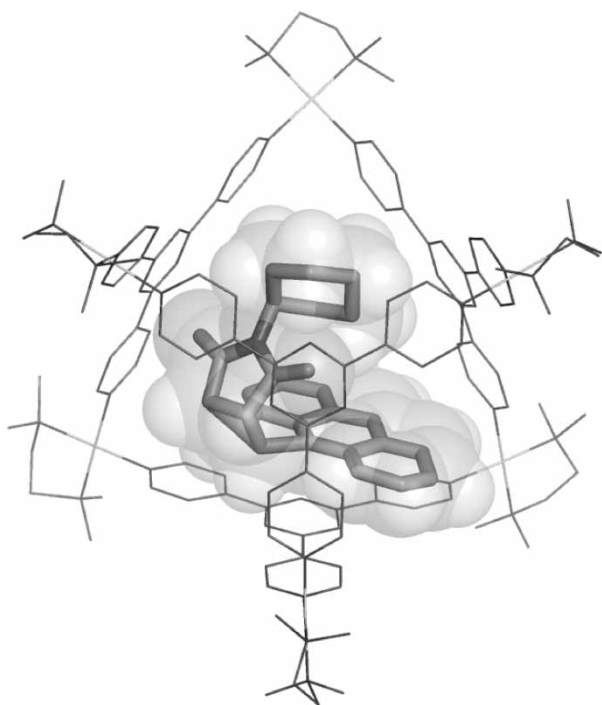
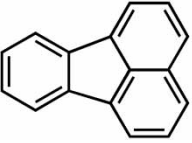
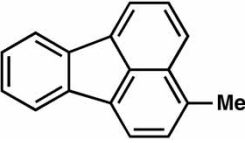
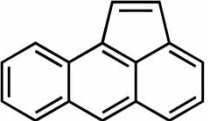
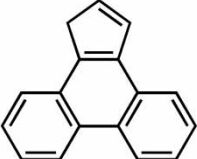


Figure 8. Crystal structure of the inclusion complex of adduct **8**. To obtain a good crystal, (tmeda)Pd(NO₃)₂ was employed instead of (en)Pd(NO₃)₂ in the formation of the cage. For clarity, H atom, anions and solvent molecules have been omitted. One of the two enantiomers is shown here. Four molecules of product **8** were equally disordered above each triazine panel ligand after symmetry operation (CCDC 746969).

Table 1. Enantiomeric excess (%) of [2 + 2] and [2 + 4] cycloadditions of aromatics with maleimide **3** within chiral cage **1b**.

Aromatic guest	[2 + 2]	[2 + 4]
 2a	40	–
 2b	50	–
 4	44	6
 5	33	26

between [2 + 2] and [2 + 4] cycloadditions is quite small in the guest pair (**3**·**5**), compared to that of pair (**3**·**4**). Presumably, because the cyclopentadiene moiety of **5** participates in both [2 + 2] and [2 + 4] cycloadditions, the resulting products have similar stereochemistry, leading to a small difference in the ee values ($\Delta ee = 7\%$). In contrast, [2 + 2] and [2 + 4] cycloadditions proceed on different rings of **4**, and the large ee difference ($\Delta ee = 38\%$) is ascribed to the shape difference between photoadduct **6** and thermal-adduct **8**. Thus, thermal agitation of the pyridine rings in cage **1** at high temperature does not significantly affect enantioselectivity of asymmetric reactions within the cage.

Enantioselectivity is determined by the population of the diastereomeric substrate pair which is suitable for the subsequent [2 + 2] or [2 + 4] cycloaddition within the chiral cage. Therefore, preorganised structure of a substrate pair within the cage is essential for achieving a high ee value.

Conclusion

The present study developed the applicable scope of asymmetric reactions within a chiral M_6L_4 cage, although the previous study was limited to [2 + 2] photoadditions with fluoranthene derivatives. In the hydrophobic cavity of the cage, owing to the pair formation of a large aromatic molecule with a round-shaped maleimide, which do not particularly interact with each other, a variety of aromatics can undergo asymmetric cycloadditions in regio- and stereo-selective manners. It is noteworthy that relatively high ee values (up to 50%) are accomplished by the chiral cage, even though the chiral centres are located far from the central reaction space. Inherent properties of the cage are maintained in the peripheral modification. Thus, 'remote chiral transfer' is a versatile and suitable strategy for cavity-directed asymmetric reactions.

Experimental

General

1H and ^{13}C NMR spectra were recorded on a Bruker DRX-500 (500 MHz) spectrometer. TMS ($CDCl_3$ solution) in a capillary served as an external standard ($\delta = 0$ ppm). CD spectra were recorded on a Jasco J-820 spectropolarimeter. IR measurements were carried out using a DIGILAB Scimitar FTS-2000 instrument. MALDI-TOF-MS data were obtained by Applied Biosystem Voyager. Melting points were determined with a Yanaco MF-500 V micro melting point apparatus. Diffraction measurements were made using a Bruker APEXII/CCD diffractometer equipped with a focusing mirror ($MoK\alpha$ radiation $\lambda = 0.71073 \text{ \AA}$). Photo irradiation was carried out with a SAN-EI Electric Co. (Osaka, Japan) UVF-352S 350-W ultra high-pressure mercury lamp. HPLC analyses were carried out using

a DAICEL chemical Industries Ltd, (Niigata, Japan), CHIRALPAC[®] IA. Solvents and reagents were purchased from TCI Co. Ltd, (Tokyo, Japan), WAKO Pure Chemical Industries Ltd, (Osaka, Japan) and Sigma-Aldrich Co. (Munich, Germany); Deuterated H_2O was acquired from Cambridge Isotope Laboratories Inc. (Andover, MA, USA) and used as supplied for the complexation reactions and NMR measurements. Aceanthrylene (**4**) was synthesised three steps from anthracene (**37**). Chiral self-assembled cage **1b** was prepared according to the already established procedure (**31**). For detailed NMR spectra of products and X-ray crystal structure of **1**·**8**, see the previous report (**32**).

Synthetic procedure and physical properties

[2 + 2] and [2 + 4] cycloadditions of aceanthrylene **4**

Aceanthrylene (**4**, 3.0 mg; 1.5×10^{-2} mmol) and *N*-cyclohexylmaleimide (**3**, 2.7 mg; 1.5×10^{-2} mmol) were suspended in a D_2O solution (1.0 mL) of cage **1a** (5.0×10^{-3} mmol; 5.0 mM) and the solution was stirred at room temperature for 1 h. After excess substrates were removed by filtration, ternary complex **1a**·(**3**·**4**) was formed in 50% yield. The solution of ternary complex **1a**·(**3**·**4**) was irradiated (400 W, high pressure mercury lamp) for 1 h at room temperature. 1H NMR analysis of the solution revealed the formation of inclusion complex **1a**·**6** in 60% yield. After decomposition of cage **1a** with HCl solution, extraction with $CHCl_3$ and purification by column chromatography ($CHCl_3$), the [2 + 2] product **6** was obtained as a pale yellow solid in 56% yield.

When the solution of ternary complex **1a**·(**3**·**4**) was stirred at $100^\circ C$ for 1 h, the colour of the solution changed from red to yellow. 1H NMR analysis of the solution revealed the formation of inclusion complex **1a**·**8** in 90% yield. After decomposition of cage **1a** with HCl solution, extraction with $CHCl_3$ and purification by column chromatography ($CHCl_3$), the [2 + 4] product **8** was isolated as a yellow solid.

A similar ternary complex **1b**·(**3**·**4**) was obtained by mixing chiral cage **1b** with **3** and **4** in water. The reactivity for [2 + 2] and [2 + 4] cycloadditions is almost the same between ternary complexes **1a**·(**3**·**4**) and **1b**·(**3**·**4**).

Compound 1a·(**3**·**4**). 1H NMR (500 MHz, D_2O , 300 K): $d = -0.26$ (br, 5H, **3**), 0.24 (br, 2H, **3**), 0.34 (br, 2H, **3**), 0.50 (br, 1H, **3**), 1.93 (br, 1H, **3**), 3.00 (s, 24H, **1a**), 5.38 (br, 1H, **4**), 5.68 (s, 2H, **3**), 5.80 (br, 1H, **4**), 5.95 (s, 1H, **4**), 5.98 (br, 1H, **4**), 6.03 (br, 1H, **4**), 6.07 (br, 1H, **4**), 6.37 (br, 1H, **4**), 6.46 (br, 1H, **4**), 6.60 (br, 1H, **4**), 8.66 (br, 24H, **1a**), 9.25 (br, 24H, **1a**).

Compound 1a·**6**. 1H NMR (500 MHz, D_2O , 300 K): $d = -2.41$ (br, 1H, **6**), -1.81 (br, 1H, **6**), -1.23 (br, 1H, **6**), -1.15 (br, 1H, **6**), -0.93 (br, 1H, **6**), -0.86 (br, 1H, **6**), -0.52 (br, 2H, **6**), 0.20 (br, 1H, **6**), 0.27 (br, 1H, **6**), 0.79

(br, 1H, **6**), 2.96 (s, 24H, **1a**), 3.02 (dd, $J = 5.0, 10.0$ Hz, 1H, **6**), 3.19 (dd, $J = 5.0, 10.0$ Hz, 1H, **6**), 3.26 (dd, $J = 5.0, 10.0$ Hz, 1H, **6**), 4.15 (dd, $J = 5.0, 10.0$ Hz, 1H, **6**), 4.23 (d, $J = 10.0$ Hz, 1H, **6**), 5.36 (s, 1H, **6**), 5.54 (t, $J = 10.0$ Hz, 1H, **6**), 5.88 (d, $J = 5.0$ Hz, 1H, **6**), 6.63 (d, $J = 10.0$ Hz, 1H, **6**), 6.97 (t, $J = 10.0$ Hz, 1H, **6**), 7.28 (t, $J = 10.0$ Hz, 1H, **6**), 8.00–9.60 (m, 48H, **1a**). Crystallographic data: CCDC 777611.

Compound 6. ^1H NMR (500 MHz, CDCl_3 , 300 K): $d = 0.22$ (br, 2H), 0.80 (br, 3H), 1.09 (m, 1H), 1.25 (br, 1H), 1.30 (br, 1H), 1.36 (br, 2H), 3.13 (tt, $J = 4.0, 12.5$ Hz, 1H), 3.84 (dd, $J = 7.0, 10.0$ Hz, 1H), 3.93 (dd, $J = 7.0, 10.0$ Hz, 1H), 4.83 (dd, $J = 7.0, 10.0$ Hz, 1H), 5.16 (dd, $J = 7.0, 10.0$ Hz, 1H), 7.30 (d, $J = 6.5$ Hz, 1H), 7.47 (t, $J = 7.0$ Hz, 1H), 7.48 (t, $J = 7.0$ Hz, 1H), 7.54 (t, $J = 7.5$ Hz, 1H), 7.77 (d, $J = 8.5$ Hz, 1H), 8.02 (d, $J = 10.5$ Hz, 1H), 8.04 (d, $J = 10.5$ Hz, 1H), 8.24 (s, 1H); ^{13}C NMR (125 MHz, CDCl_3 , 300 K): $d = 24.6$ (CH_2), 25.4 (CH_2), 25.5 (CH_2), 27.3 (CH_2), 27.4 (CH_2), 41.7 (CH), 42.3 (CH), 43.8 (CH), 44.8 (CH), 50.9 (CH), 120.3 (CH), 123.4 (CH), 123.8 (CH), 125.3 (CH), 125.4 (CH), 125.7 (CH), 127.6 (CH), 127.9 (C), 129.2 (CH), 129.4 (C), 133.7 (C), 137.8 (C), 140.3 (C), 142.1 (C), 176.2 (C), 176.4 (C); MALDI-TOF-MS m/z calcd for $[\text{M}]^+$: 381.17, found 381.38; IR (ATR, cm^{-1}): 2936, 2857, 1767, 1695, 1450, 1394, 1372, 1346, 1259, 1200, 1190, 1170, 1123; mp: $> 230^\circ\text{C}$ (decomposed); EA calcd for $\text{C}_{26}\text{H}_{23}\text{NO}_2 \cdot \text{H}_2\text{O}$: C, 78.17; H, 6.31; N, 3.51. Found: C, 77.91; H, 5.96; N, 3.30.

Compound 1a·8. ^1H NMR (500 MHz, D_2O , 300 K): $d = -2.14$ (br, 1H, **8**), -1.97 (br, 1H, **8**), -1.16 (br, 2H, **8**), -0.91 (br, 1H, **8**), -0.84 (br, 2H, **8**), -0.39 (br, 2H, **8**), 0.04 (br, 1H, **8**), 0.90 (br, 1H, **8**), 2.11 (br, 1H, **8**), 2.10–2.30 (m, 2H, **8**), 2.70–2.85 (m, 1H, **8**), 2.90 (s, 24H, **1a**), 4.12 (d, $J = 5.0$ Hz, 1H, **8**), 4.80 (br, 1H, **8**), 4.97 (s, 1H, **8**), 5.57 (t, $J = 5.0$ Hz, 1H, **8**), 5.98 (d, $J = 5.0$ Hz, 1H, **8**), 6.15 (d, $J = 10.0$ Hz, 1H, **8**), 6.33 (t, $J = 10.0$ Hz, 1H, **8**), 6.45 (t, $J = \text{Hz}$, 1H, **8**), 8.40–9.70 (m, 48H, **1a**). Crystallographic data: CCDC 746969.

Compound 8. ^1H NMR (500 MHz, CDCl_3 , 300 K): $d = 0.10$ – 0.20 (m, 1H), 0.33– 0.44 (m, 1H), 0.70– 0.90 (m, 2H), 1.20– 1.40 (m, 3H), 1.25– 1.40 (m, 3H), 3.12 (dd, $J = 4.0, 9.0$ Hz, 1H), 3.15 (dd, $J = 4.0, 9.0$ Hz, 1H), 3.30 (tt, $J = 4.0, 12.5$ Hz, 1H), 4.54 (br, 1H), 4.82 (br, 1H), 6.73 (t, $J = 7.5$ Hz, 1H), 6.78 (t, $J = 7.5$ Hz, 1H), 7.07 (d, $J = 5.0$ Hz, 1H), 7.16 (d, $J = 5.0$ Hz, 1H), 7.45 (t, $J = 7.5$ Hz, 1H), 7.55 (s, 1H), 7.61 (d, $J = 7.5$ Hz, 1H), 7.69 (d, $J = 7.5$ Hz, 1H); ^{13}C NMR (125 MHz, CDCl_3 , 300 K): $d = 24.7$ (CH_2), 25.4 (2CH_2), 27.2 (CH_2), 27.6 (CH_2), 39.3 (CH), 42.5 (CH), 46.0 (2CH), 51.0 (CH), 122.3 (CH), 123.9 (CH), 126.1 (CH), 126.6 (C), 127.0

(CH), 127.4 (CH), 130.2 (CH), 134.5 (C), 134.9 (CH), 135.4 (C), 136.2 (CH), 138.9 (C), 139.4 (C), 176.9 (C), 177.1 (C); MALDI-TOF-MS m/z calcd for $[\text{M}]^+$: 381.17, found 381.30; IR (ATR, cm^{-1}): 2932, 2857, 1769, 1698, 1397, 1372, 1346, 1259, 1198, 1147; mp: 168– 169°C ; EA calcd for $\text{C}_{26}\text{H}_{23}\text{NO}_2 \cdot 0.5\text{H}_2\text{O}$: C, 79.97; H, 6.20; N, 3.59. Found: C, 79.65; H, 6.22; N, 3.33.

[2 + 2] and [2 + 4] cycloadditions of 1H-cyclopenta[1]phenanthrene 5

1H-Cyclopenta[1]phenanthrene (**5**, 3.2 mg; 1.5×10^{-2} mmol) and *N*-cyclohexylmaleimide (**3**, 2.7 mg; 1.5×10^{-2} mmol) were suspended in a D_2O solution (1.0 mL) of cage **1a** (5.0×10^{-3} mmol; 5.0 mM), and the solution was stirred at room temperature for 1 h. After excess substrates were removed by filtration, ternary complex **1a·(3·5)** was obtained in 30% yield. The solution of ternary complex **1a·(3·5)** was irradiated (400 W, high pressure mercury lamp) for 15 min at room temperature. ^1H NMR analysis of the solution revealed the formation of inclusion complex **1a·7** in 50% yield. Only single isomer **7** was formed in the cavity of cage **1a**, but the escape of the substrates from the cage under the reaction conditions reduced the product yield. After decomposition of cage **1a** with HCl solution, extraction with CHCl_3 and purification by column chromatography (CHCl_3), the [2 + 2] product **7** was obtained as a white solid.

On stirring the solution of ternary complex **1a·(3·5)** at 100°C for 1 h, the colour of the solution changed from yellow to pale yellow. ^1H NMR analysis of the solution revealed the formation of inclusion complex **1a·9** in 95% yield. After extraction with CHCl_3 and purification by column chromatography (CHCl_3), the [2 + 4] product **9** was obtained as a white solid in 71% yield.

A similar ternary complex **1b·(3·5)** was obtained by mixing chiral cage **1b** with **3** and **5** in water. The reactivity for [2 + 2] and [2 + 4] cycloadditions is almost the same between ternary complexes **1a·(3·4)** and **1b·(3·4)**.

Compound 1a·(3·5). ^1H NMR (500 MHz, D_2O , 300 K): $d = -0.38$ (br, 2H, **3**), -0.25 (br, 2H, **3**), -0.15 (br, 2H, **3**), 0.27 (br, 4H, **3**), 0.64 (br, 1H, **3**), 1.73 (br, 1H, **5**), 1.82 (br, 1H, **3**), 2.89 (s, 24H, **1a**), 5.24 (br, 1H, **5**), 5.47 (s, 2H, **3**), 5.59 (br, 1H, **5**), 5.67 (br, 1H, **5**), 5.85 (br, 1H, **5**), 6.05 (br, 1H, **5**), 6.11 (br, 1H, **5**), 6.21 (br, 1H, **5**), 6.37 (br, 1H, **5**), 6.53 (br, 2H, **5**), 8.20– 9.50 (br, 48H, **1a**).

Compound 1a·7. ^1H NMR (500 MHz, D_2O , 300 K): $d = -2.36$ (d, $J = 8.0$ Hz, 1H, **7**), -1.29 (d, $J = 10.0$ Hz, 2H, **7**), -1.15 (q, $J = 7.5$ Hz, 1H, **7**), -1.05 (q, $J = 8.0$ Hz, 1H, **7**), -0.73 (q, $J = 10.0$ Hz, 1H, **7**), -0.62 (q, $J = 11.5$ Hz, 1H, **7**), -0.38 (q, $J = 14.0$ Hz, 1H, **7**), 0.14 (d, $J = 9.5$ Hz, 1H, **7**), 0.53 (d, $J = 11.0$ Hz, 1H,

7), 0.73 (q, $J = 9.0$ Hz, 1H, **7**), 0.99 (m, 1H, **7**), 1.39 (d, $J = 14.0$ Hz, 1H, **7**), 2.96 (s, 24H, **1a**), 3.22 (q, $J = 9.0$ Hz, 1H, **7**), 3.54 (t, $J = 9.0$ Hz, 1H, **7**), 4.81 (m, 1H, **7**), 5.39 (d, $J = 7.5$ Hz, 1H, **7**), 5.90 (d, $J = 8.0$ Hz, 1H, **7**), 6.12 (d, $J = 8.0$ Hz, 1H, **7**), 6.39 (t, $J = 8.0$ Hz, 1H, **7**), 6.85 (t, $J = 7.5$ Hz, 1H, **7**), 7.02 (t, $J = 7.5$ Hz, 1H, **7**), 7.23 (t, $J = 7.5$ Hz, 1H, **7**), 8.10–9.70 (m, 48H, **1a**).

Compound 7. ^1H NMR (500 MHz, CDCl_3 , 300 K): $d = 0.35$ – 0.45 (m, 2H), 0.70–0.90 (m, 3H), 1.20 (br, 1H, H_t), 1.20–1.35 (m, 3H), 1.40–1.50 (m, 1H), 3.33 (m, 2H), 3.46 (dd, $J = 3.0, 10.0$ Hz, 1H), 3.68 (d, $J = 12.5$ Hz, 1H), 3.83 (m, 2H), 4.85 (t, $J = 7.5$ Hz, 1H), 7.62 (m, 4H), 7.80 (d, $J = 10.0$ Hz, 1H), 7.87 (d, $J = 10.0$ Hz, 1H), 8.61 (d, $J = 10.0$ Hz, 1H), 8.64 (d, $J = 10.0$ Hz, 1H); ^{13}C NMR (125 MHz, CDCl_3 , 300 K): $d = 24.6$ (CH_2), 25.4 (CH_2), 25.5 (CH_2), 27.3 (CH_2), 27.9 (CH_2), 34.1 (CH_2), 36.1 (CH), 40.3 (CH), 43.3 (CH), 46.6 (CH), 51.1 (CH), 122.7 (CH), 123.0 (CH), 125.5 (CH), 126.3 (CH), 126.4 (CH), 126.5 (CH), 126.6 (CH), 126.8 (CH), 129.0 (C), 129.3 (C), 130.5 (C), 131.0 (C), 134.6 (C), 139.9 (C), 177.0 (C), 177.3 (C); MALDI-TOF-MS m/z calcd for $[\text{M}]^+$: 395.19, found 395.60; IR (ATR, cm^{-1}): 2932, 2857, 1764, 1692, 1450, 1393, 1370, 1346, 1183, 1129; mp: $> 230^\circ\text{C}$ (decomposed); EA calcd for $\text{C}_{27}\text{H}_{25}\text{NO}_2 \cdot 0.5\text{H}_2\text{O}$: C, 80.17; H, 6.48; N, 3.46. Found: C, 79.92; H, 6.39; N, 3.22.

Compound 1a·9. ^1H NMR (500 MHz, D_2O , 300 K): $d = -1.61$ (br, 1H, **9**), -1.24 (br, 1H, **9**), -1.05 (br, 1H, **9**), -0.85 (br, 1H, **9**), -0.35 (m, 2H, **9**), -0.12 (m, 1H, **9**), 0.40 (m, 1H, **9**), 0.65 (m, 1H, **9**), 0.72 (m, 1H, **9**), 1.12 (m, 2H, **9**), 2.62 (m, 1H, **9**), 2.90 (s, 24H, **1a**), 2.99 (m, 1H, **9**), 3.95 (m, 1H, **9**), 4.25 (s, 1H, **9**), 5.15 (d, 1H, **9**), 5.24 (d, 1H, **9**), 5.60 (m, 1H, **9**), 6.30 (m, 1H, **9**), 6.50 (m, 1H, **9**), 6.58 (m, 1H, **9**), 7.00 (m, 1H, **9**), 8.10–9.80 (m, 48H, **1a**).

Compound 9. ^1H NMR (500 MHz, CDCl_3 , 300 K): $d = 0.88$ (t, $J = 7.0$ Hz, 1H), 1.03 (t, $J = 13.0$ Hz, 1H), 1.15 (q, $J = 6.5$ Hz, 2H), 1.28 (m, 1H), 1.49–1.61 (m, 3H), 1.88 (q, $J = 12.5$ Hz, 1H), 1.94 (d, $J = 8.5$ Hz, 1H), 2.36 (d, $J = 8.5$ Hz, 1H), 3.30 (d, $J = 7.5$ Hz, 1H), 3.54 (q, $J = 4.5$ Hz, 1H), 3.60 (m, 1H), 3.70 (br, 1H), 6.59 (d, $J = 3.0$ Hz, 1H), 7.21 (t, $J = 7.5$ Hz, 1H), 7.34 (t, $J = 7.5$ Hz, 1H), 7.36 (t, $J = 7.5$ Hz, 1H), 7.38 (d, $J = 7.5$ Hz, 1H), 7.42 (t, $J = 7.5$ Hz, 1H), 7.49 (d, $J = 7.5$ Hz, 1H), 8.01 (d, $J = 7.5$ Hz, 1H), 8.03 (d, $J = 7.5$ Hz, 1H); ^{13}C NMR (125 MHz, CDCl_3 , 300 K): $d = 24.8$ (CH_2), 25.7 (2CH_2), 28.4 (2CH_2), 45.5 (CH), 45.9 (CH), 51.1 (CH), 52.5 (CH), 57.1 (C), 60.6 (CH_2), 123.8 (CH), 124.0 (2CH), 124.5 (CH), 126.1 (CH), 127.3 (C), 127.5 (CH), 127.8 (CH), 128.1 (CH), 129.2 (CH), 132.1 (C), 133.2 (C), 135.8 (C), 142.5 (C), 175.3 (C), 177.3 (C); MALDI-TOF-MS m/z calcd for $[\text{M}]^+$: 395.19,

found 395.40; IR (ATR, cm^{-1}): 2934, 2857, 1759, 1690, 1448, 1371, 1259, 1190, 1150, 1048; mp: 160–162°C; EA calcd for $\text{C}_{27}\text{H}_{25}\text{NO}_2 \cdot 0.5\text{H}_2\text{O}$: C, 80.17; H, 6.48; N, 3.46. Found: C, 80.39; H, 6.52; N, 3.21.

HPLC analyses

Asymmetric [2 + 2] photo-cycloadditions of aromatic compounds **4** and **5** with maleimide **3** within chiral cage **1b** were carried out by irradiation with high-pressure Hg lamp. For control experiments, cage **1b'** with the inverse chiral auxiliaries ((1*S*, 2*S*)-*N,N'*-1,2-diaminocyclohexane derivatives) on each Pd centre was also prepared. Racemic products obtained within achiral cage **1a** were also used as references. After irradiation, the products were extracted with chloroform and the solution (*ca.* 20 μL) was injected to the HPLC system connected with a chiral column (DAICEL CHIRALPAK[®] IA). The developing solvent mixture was of chloroform and hexane (1:4). Retention times of enantiomers: 17.2 and 20.0 min (**6**); 11.8 and 16.2 min (**7**), 12.9 and 15.2 min (**8**); 20.4 and 40.2 min (**9**).

Supplementary materials

NMR spectra, HPLC analytical data, and crystallographic data are available as Supplementary materials, online.

Acknowledgements

This research was supported in part by the Global COE Program (Chemistry Innovation through Cooperation of Science and Engineering), MEXT, Japan.

Notes

1. The remaining 50% is a dimer formation of maleimide **3** within the cage, $\mathbf{1} \cdot (\mathbf{3})_2$.
2. The conversion is almost 100% as starting compounds and any by-products were not extracted from the cage after the reaction. The moderate yield (60%) is due to escape of the substrates from the cage under the reaction conditions.

References

- (1) Hembury, G.A.; Borovkov, V.V.; Inoue, Y. *Chem. Rev.* **2008**, *108*, 1–73.
- (2) Koblenz, T.S.; Wassenaar, J.; Reek, J.N.H. *Chem. Soc. Rev.* **2008**, *37*, 247–262.
- (3) Vriezema, D.M.; Aragonès, M.C.; Elemans, J.A.A.W.; Cornelissen, J.J.L.M.; Rowan, A.E.; Nolte, R.J.M. *Chem. Rev.* **2005**, *105*, 1445–1490.
- (4) Breslow, R.; Dong, S.D. *Chem. Rev.* **1998**, *98*, 1997–2012.
- (5) Takahashi, K. *Chem. Rev.* **1998**, *98*, 2013–2034.
- (6) Rao, V.P.; Turro, N.J. *Tetrahedron Lett.* **1989**, *30*, 4641–4644.
- (7) Shailaja, J.; Karthikeyan, S.; Ramamurthy, V. *Tetrahedron Lett.* **2002**, *43*, 9335–9339.
- (8) Pattabiraman, M.; Natarajan, A.; Kaanumalle, L.S.; Ramamurthy, V. *Org. Lett.* **2005**, *7*, 529–532.
- (9) Fleck, M.; Yang, C.; Wada, T.; Inoue, Y.; Bach, T. *Chem. Commun.* **2007**, 822–824.

- (10) Yang, C.; Mori, T.; Inoue, Y. *J. Org. Chem.* **2008**, *73*, 5786–5794.
- (11) Yang, C.; Mori, T.; Origane, Y.; Ko, Y.H.; Selvapalam, N.; Kim, K.; Inoue, Y. *J. Am. Chem. Soc.* **2008**, *130*, 8574–8575.
- (12) Lu, R.; Yang, C.; Cao, Y.; Tong, L.; Jiao, W.; Wada, T.; Wang, Z.; Mori, T.; Inoue, Y. *J. Org. Chem.* **2008**, *73*, 7695–7701.
- (13) Ke, C.; Yang, C.; Mori, T.; Wada, T.; Liu, Y.; Inoue, Y. *Angew. Chem. Int. Ed.* **2009**, *48*, 6675–6677.
- (14) Fukuhara, G.; Mori, T.; Inoue, Y. *J. Org. Chem.* **2009**, *74*, 6714–6727.
- (15) Yang, C.; Inoue, Y. In *Cyclodextrin Materials Photochemistry, Photophysics and Photobiology*; Douhal, A., Ed.; Elsevier: New York, 2006; Chapter 11, pp 241–266.
- (16) Buschmann, H.; Scharf, H.D.; Hoffmann, N.; Plath, M.W.; Runsink, J. *J. Am. Chem. Soc.* **1989**, *111*, 5367–5373.
- (17) Buschmann, H.; Scharf, H.-D.; Hoffmann, N.; Esser, P. *Angew. Chem. Int. Ed. Engl.* **1991**, *30*, 477–515.
- (18) Clayden, J.; Knowles, F.E.; Menet, C.J. *J. Am. Chem. Soc.* **2003**, *125*, 9278–9279.
- (19) Tsutsumi, K.; Nakano, H.; Furutani, A.; Endou, K.; Merpuge, A.; Shintani, T.; Morimoto, T.; Kakiuchi, K. *J. Org. Chem.* **2004**, *69*, 785–789.
- (20) Hoffmann, N. *Chem. Rev.* **2008**, *108*, 1052–1103.
- (21) Hoffmann, N.; Pete, J.-P. In *Chiral Photochemistry (Molecular and Supramolecular Photochemistry)*; Inoue, Y., Ramamurthy, V., Eds.; Marcell Dekker: New York, 2004; Vol. 11, pp 179–233.
- (22) Davis, A.V.; Fiedler, D.; Ziegler, M.; Terpin, A.; Raymond, K.N. *J. Am. Chem. Soc.* **2007**, *129*, 15354–15363.
- (23) Fiedler, D.; vanHalbeek, H.; Bergman, R.G.; Raymond, K.N. *J. Am. Chem. Soc.* **2006**, *128*, 10240–10252.
- (24) Hastings, C.J.; Fiedler, D.; Bergman, R.G.; Raymond, K.N. *J. Am. Chem. Soc.* **2008**, *130*, 10977–10983.
- (25) Brown, C.J.; Bergman, R.G.; Raymond, K.N. *J. Am. Chem. Soc.* **2009**, *131*, 17530–17531.
- (26) Castellano, R.K.; Kim, B.H.; Rebek, J. Jr. *J. Am. Chem. Soc.* **1997**, *119*, 12671–12672.
- (27) Castellano, R.K.; Nuckolls, C.; Rebek, J. Jr. *J. Am. Chem. Soc.* **1999**, *121*, 11156–11163.
- (28) Amaya, T.; Rebek, J. Jr. *J. Am. Chem. Soc.* **2004**, *126*, 6216–6217.
- (29) Schramm, M.P.; Restorp, P.; Zelder, F.; Rebek, J. Jr. *J. Am. Chem. Soc.* **2008**, *130*, 2450–2451.
- (30) Scarso, A.; Shivanyuk, A.; Hayashida, O.; Rebek, J. Jr. *J. Am. Chem. Soc.* **2003**, *125*, 6239–6243.
- (31) Nishioka, Y.; Yamaguchi, T.; Kawano, M.; Fujita, M. *J. Am. Chem. Soc.* **2008**, *130*, 8160–8161.
- (32) We have recently found that aromatic compounds **4** and **5** undergo the both [2 + 2] and [2 + 4] cycloadditions within achiral cage **1a**. Horiuchi, S.; Nishioka, Y.; Murase, T.; Fujita, M. *Chem. Commun.* **2010**, *46*, 3460–3462.
- (33) Yoshizawa, M.; Tamura, M.; Fujita, M. *J. Am. Chem. Soc.* **2004**, *126*, 6846–6847.
- (34) Schneider, N.; Huttenloch, M.E.; Stehling, U.; Kirsten, R.; Schaper, F.; Brintzinger, H.H. *Organometallics* **1997**, *16*, 3413–3420.
- (35) Rigby, S.S.; Decken, A.; Bain, A.D.; McGlinchey, M.J. *J. Organomet. Chem.* **2001**, *637–639*, 372–381.
- (36) Rigby, S.S.; Stradiotto, M.; Brydges, S.; Pole, D.L.; Top, S.; Bain, A.D.; McGlinchey, M.J. *J. Org. Chem.* **1998**, *63*, 3735–3740.
- (37) Becker, H.D.; Hansen, L. *J. Org. Chem.* **1985**, *50*, 277–279.